Preparation and Electrical Characterization of Poly(vinyl amine) Hydrogels, Crosslinked with Cu(II) Ions, and Evaluation of Their Potentiality as Water Sensor Material

Jesus G. Mendoza-Payan, Sergio Flores-Gallardo, Alfredo Marquez-Lucero

Centro de Investigación en Materiales Avanzados (CIMAV), CONACYT, Miguel Cervantes 120, Complejo Industrial Chihuahua, Chihuahua, Chih. 31109, CP, Mexico

Received 11 November 2008; accepted 11 July 2009
DOI 10.1002/app.31097
Published online 10 September 2009 in Wiley InterScience (www.interscience.wiley.com).

ABSTRACT: A method to prepare water sensitive composites employing crosslinked poly(vinyl amine) (PVAm) and Cu(II) ions as reticulation agent is disclosed in this work. This article presents in detail, the reticulation reaction and its pH dependence, as well as its electrical, rheological, and thermal properties of the PVAm-Cu(II) composites obtained. The complex bonds formed between the Cu(II) ions and the amine groups of PVAm produce an interesting network of crosslinked structures that generate a microporous morphology when the material is extruded. This characteristic favors fast absorption of water when it is wetted, and a concomitant decrease in its apparent resistivity in a very short period of time. Furthermore, they present an excellent thermal stability and suitable processability. These characteristics make them interesting candidates to design ultra fast water sensors. © 2009 Wiley Periodicals, Inc. J Appl Polym Sci 115: 790–801, 2010

Key words: polymer science and technology; polymeric metal complexes; crosslinked hydrogels; water sensors

INTRODUCTION

The issue of water economy is becoming a critical problem in urban centers as well as in agricultural districts because of the increasing price of this essential resource. In this context, leakages from water pipes are the object of much attention from administrations and companies in charge of water supply. However, considerable efforts are still necessary to obtain a satisfactory service quality. Among many similar examples, the case of Mexico City is interesting since the loss of water through leakages in this capital is about 25% of the total amount of the water consumption. Unexpectedly, the investigation of this matter in terms of amounts, causes, and solutions revealed that such a problem is worldwide, and that it definitely received insufficient attention in the past because of the abundance of water in developed countries and the absence of low-cost remedies in emerging countries. Because of the exponential increase of water price everywhere and the dramatic shortage in many regions of the world, the development of efficient leakage sensors becomes a high-priority issue. As such, the latter controls the capability to fix rapidly the water loss in the ground and avoid the damage in surrounding infrastructures.

To monitor newly installed water pipes, a "distributed" design is a cheap and reliable solution for the detection of leaks.[1] A linear sensor is placed along the pipe that contains: (i) A polymeric material whose electrical properties change when it enters in contact with water, (ii) an electrical conductor that senses the change in the material's property and, (iii) a distant monitoring system that measures the position of electric perturbation. When a leak occurs near the sensor, water permeates into the material and its electrical resistance drops. This effect triggers an alarm which warns the monitoring system that a leak has occurred and alerts of a leak.

To produce sensors as the ones described above, hydrogels crosslinked with no traditional methods can be currently employed. Poly(vinyl amine) (PVAm) is a polymer with interesting properties for those purposes. Indeed, when softly crosslinked PVAm becomes a hydrogel that is capable of absorbing a large quantity of water without dissolving. This polymer can be crosslinked employing a method based on a chelating reaction with copper ions.[2,3] The coordinated covalent bonds formed between the Cu^{2+} ions and the amine groups of PVAm produce chain junctures with limited density,[4] to obtain certain properties such as: (i) significant swelling upon water absorption, (ii) resistance to dissolution in water, (iii) ability of extrusion processing, (iv) excellent thermal and chemical stability

Correspondence to: A. Marquez-Lucero (alfredo.marquez@cimav.edu.mx).

Contract grant sponsors: CONACyT and SNI.

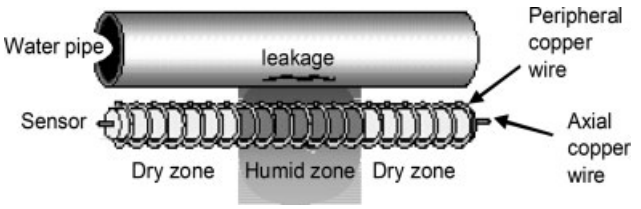

Figure 1 Scheme of the water leakage sensor.[1]

and, (v) low electric resistivity in the wet state. We have taken advantage of those properties to design distributed water sensors with ultra fast response, which may be utilized for the detection of leakages along water pipes, as well as to monitor places that must be free of water leaks as; libraries, electrical control centers, boats, ships, submarine facilities, etc.

A sensor representation is shown in Figure 1. The details of monitoring and pinpointing system coupled to this sensor; as well as the method used to differentiate a water leak from a pipeline and from filtration of rainwater is not considered in the present work, the focus is on proposing a polymeric material with excellent properties for application in distributed water sensors. However, the previous details can be consulted in Marquez and Mendoza patent application.[1]

EXPERIMENTAL

Materials

The hydrogel PVAm used in this work was a commercial polymer provided by BASF under the commercial name lupamin 9095.[5] This polymer was obtained by hydrolysis of poly(vinyl formamide) according to supplier information. In the as-received form, the neat hydrogel is presented under the form of an aqueous solution with a concentration of 22.3 wt % polymer. The average molecular weight of the polymer, according to the supplier technical specifications, is 340,000 g/mol and density equal to 1.08 ± 0.001 g/mL. The viscosity and pH of the aqueous polymer solution was equal to 8.5 ± 0.015 Pa s and 5.0 ± 0.1 respectively.

Cupric sulfate, $CuSO_4$, obtained from JT-Baker as a pentahydrated analytic grade, was employed as crosslinking agent for PVAm. Also hydrochloric acid, HCl, and sodium hydroxide, NaOH, were utilized to control the crosslinking reaction. The former is a 36.5% solution from Sigma Aldrich, and the latter a 10 M solution prepared from caustic soda by JT-Baker. Finally, 1, 2, 3 propanetriol by Sigma Aldrich was used as plasticizer.

Methods

The crosslinking reaction between PVAm and $CuSO_4$ could not be performed by simply pouring the copper salt powder into the as-received polymer solution because an instantaneous and fast crosslinking reaction occurs if cupric sulfate is added without previous control of the pH solution. The crosslinking reaction generates the rise of the solution viscosity hindering correct dispersion of the copper salt and consequently an inhomogeneous crosslinking. Therefore, to control this effect, the PVAm solution was carried out at a low pH level to protonate the amine groups. The protonation of those groups prevents them from reacting with the copper salt immediately. In this condition, cupric sulfate was homogeneously dispersed into the solution. Subsequently, the pH was increased to a value which permitted the copper salt to react.

To evaluate the density of amine groups and acid-base parameters of the PVAm, a potentiometric titration was performed as follows: An aliquot of PVAm solution (5 mL; 22.30% w/w) was titrated with 20 mL of hydrochloric acid (0.279*M*). Subsequently, the resultant solution was dried by convection employing N_2 during 24 h to remove the water and excess of hydrochloric acid. Afterward, the remaining solid was dissolved in 50 mL of distillated water and titrated with NaOH (0.30*M*) employing a precision burette at 25°C, the pH was monitored with a Corning 2095 pH-meter equipped with a Thermo–Orion 9110600 glass electrode. The ionic force of the system was regulated employing KCl with a concentration equal to 1*M*.

The transition of the protonated and unprotonated states of the amine group is described by eq. (1):

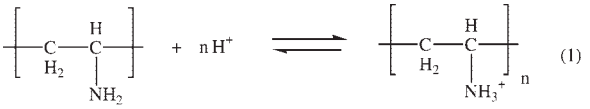

(1)

Moreover, it is possible to predict the protonated amine group molar fraction F_p along the titration curve as a function of pH using the following expression[6]:

$$F_p = \frac{[\mathrm{PV-NH_3^+}]}{[\mathrm{PV-NH_2}] + [\mathrm{PV-NH_3^+}]} = \frac{10^{-\mathrm{pH}}}{10^{-\mathrm{pH}} + 10^{-\mathrm{p}K_a}} \quad (2)$$

Where, [PV–NH_2] and [PV–NH_3^+] are the molar concentrations (mol/L) of vinyl amine units of the PVAm in their unprotonated and protonated forms, respectively. The parameter pK_a is the apparent acid dissociation constant described by modified Henderson–Hasselbach model[6–9]:

TABLE I
Formulations of Three Solutions with Different Content of Cupric Sulfate. After the Crosslinking Reaction Those Formulations Were Dried and Extruded

Formulations	PVAm matrix (wt %)	Cupric sulfate crosslinking agent (wt %)	HCl (wt %)	NaOH (wt %)	Water (wt %)
A	15.61	0.07	4.34	4.76	70.00
B	15.90	0.25	4.43	4.86	69.12
C	15.51	0.50	4.37	4.80	69.53

$$\mathrm{pH} = \mathrm{p}K_a + m\mathrm{Log}\left(\frac{\alpha}{1-\alpha}\right) \quad (3)$$

Where, the parameter m is a measure of the electrostatic interaction between neighboring amine groups, and α is the ionization degree. To establish the evolution of the protonated fraction during the crosslinking reaction, this progress was analyzed by means of viscosity measurements. A PVAm solution (100 mL, 15% w/w) was acidified with hydrochloric acid until pH = 1 and subsequently 0.1 g of cupric sulfate was added to solution. The solution was mixed until a homogeneous dispersion was obtained. Then, the pH was increased gradually by addition of NaOH 0.20*M*; the viscosity was measured employing a Couette rheometer (Brookfield RDVD) at the same time period.

Once the previous evaluation has been done and optimal conditions were determined, samples of PVAm–Cu complex were prepared with different proportions of cupric sulfate (tested formulations are reported in the Table I).

The composites were extruded in a Brabender single-screw laboratory extruder (Type 2523) at a temperature of 140°C, employing a ribbon and a coating die. Two different types of samples were prepared employing the previous composites which we will describe later.

To measure the percentage of gel, before and after extrusion processing, the next test was carried out three times as follows: a 5 g sample was placed in a cellulose thimble. The thimble was put in a Soxhlet extractor using distillated water as the reflux fluid. Then the Soxhlet extractor was run for 6 h. The remaining gel deposited in the thimble was dried and weighed. Using this data, the gel fraction was calculated. Employing the previous samples, free of unlinked fraction, we measured their crosslinked density by means of the following method; samples of 3 g with disk geometry (3 cm in diameter and 0.5 cm in height) were dried during 6 h at 105°C for their subsequent placement in a previously dehumidified and stabilized cellulose thimble. Subsequently, the samples were immersed in water. The water weight uptake was measured every 10 min. Finally, the volume fraction of polymer in network equilibrium ϕ, defined as the ratio of dry gel volume to swollen gel volume $\phi = V_0/V_f$, was calculated. Now, the crosslinked density,[10] ρ_c, is defined as:

$$\rho_c = \mathrm{M}_0/\mathrm{M}_c \quad (4)$$

Where M_0 is the molecular weight per structural unit and M_c the molecular weight per crosslinked unit. Following Flory's theory,[10] ρ_c is related to molecular microstructure through eq. (5):

$$\rho_c = -\frac{M_0}{\rho}\,\frac{\ln(1-\phi)+\phi+\chi_{12}\phi}{V_l(\phi^{1/3}-\phi)} \quad (5)$$

Where χ_{12} is the Flory interaction parameter, V_1 the solvent molar volume and ρ the hydrogel density.

The polymer–solvent interaction parameter, χ_{12}, was calculated by viscosimetry at theta temperature. The theta temperature is the temperature at which the coiled polymer molecules become Gaussian distributed. At this condition, the second viral coefficient is practically negligible, and a reference intrinsic viscosity $[\eta]_\theta$ may be evaluated.[11] Intrinsic viscosity $[\eta]$ have been determined employing the relative and specific viscosities defined by Flory,[10] and using the Kraemer (6) and Huggins (7) linear relationships.

$$\frac{\eta_{sp}}{c} = [\eta] + K_H[\eta]^2 c \quad (6)$$

$$\frac{\ln \eta_r}{c} = [\eta] + K_k[\eta]^2 c \quad (7)$$

Where c is the concentration of polymer solution, $[\eta]$ is the intrinsic viscosity, K_k and K_H are the Kraemer and Huggins coefficients, respectively. Intrinsic viscosity is assessed at the common intercept of the Kraemer and Huggins experimental straight lines.[11] Finally, the Flory interaction parameter can be calculated by the following equation[12]:

$$\chi_{12} = \frac{1}{2} - \frac{[\eta]-[\eta]_\theta}{2.10\left(\frac{3}{2\pi}\right)^{3/2}\left(\frac{\Phi_0}{N_A}\right)\left(\frac{M_2\upsilon_2^2}{V_1}\right)} \quad (8)$$

where Φ_0 is the universal viscosity constant equal to 2.5×10^{-21} mol^{-1}; M_2 is the polymer average molecular weight; υ_2 is partial specific volume of the polymer and N_A is Avogadro's number. Finally, the theta temperature is determined where Kraemer plot ($\ln(\eta_r/c)$ versus c) has minimal slope.[13]

To perform the previous measures, special samples were prepared dissolving the dry polymer with distilled water obtaining solutions with concentrations between 6 g/dL and 1 g/dL. The

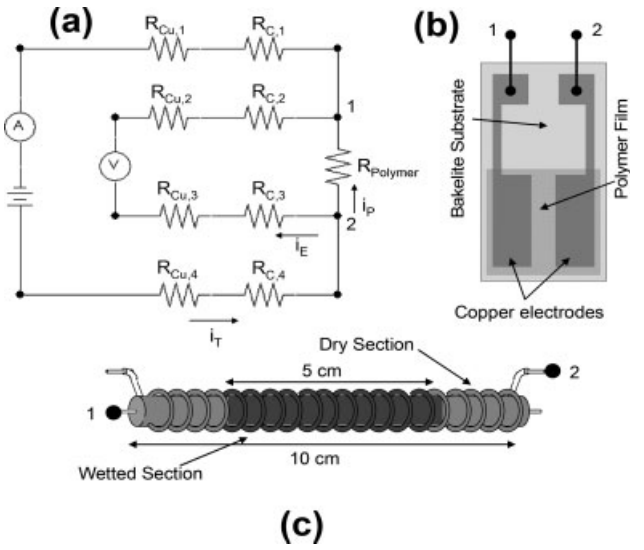

Figure 2 System and description of four probes electrical resistance tests. (a) Equivalent circuit of the involved elements at the measurement (the samples were connected to electrodes 1 and 2). (b) Type I test, the sample is connected to the previous circuit at the electrodes 1 and 2. (c) Type II test the sample is connected to the previous circuit at the electrodes 1 and 2.

measurements were carried out in an Ubbelohode 3b type capillary viscosimeter. Each sample was introduced into a viscosimeter, immersed in an isothermal water bath adjusting the temperature to 35, 30, 25, and 20°C ± 0.10. The measures were carried out in thermal equilibrium.

Subsequently, samples from formulations described in Table I were analyzed by infrared spectroscopy (Perkin Elmer model 8400) and thermogravimetric analysis (TGA-DTA TA Instruments, model SDT 2960). The viscosity of the dry hydrogels was evaluated at a processing temperature of 140°C using a Haake RS-75 rheometer, with cone-plate geometry. Also, the samples surface was inspected by scanning electron microscopy (Jeol model JSM 5800-LV).

As previously mentioned two types of samples were extruded. Both types electrically tested employing a four probes circuit [Fig. 2(a)]. The first type [Fig. 2(b)] was designed to evaluate the physical, chemical, and electrical properties of the material, whereas the second one [Fig. 2(c)] was designed to evaluate the material performance in a sensor prototype. The electrical resistivity of those samples was evaluated in their dry and wet states by mean of Kelvin–Four probes technique[14] employing an Agilent 34401 A multimeter [Fig. 2(a)]. The samples were prepared as follows: For Type I test, a Bakelite substrate (1 cm × 2 cm) with two silver electrodes (64 mm^2) was coated with an extruded PVAm-Cu(II) strip of 1.5 mm in thickness, as illustrated in Figure 2(b). For Type II test a copper wire, 0.5 mm in diameter, was coated by coextrusion with a 1.5 mm layer of PVAm-Cu(II). Subsequently, another copper wire was helicoidally wound along the extruded cable as shown in Figure 2(c). In this last case, samples had 10 cm in length but only their central zone of 5 cm was dipped in water.

RESULTS AND DISCUSSION

Figure 3(a) shows the potentiometric curve of the protonated PVAm, where we can observe just one inflection point. This is an unexpected result because some authors reported titrations of PVAm by Carbon-13 and Nitrogen-15 NMR pH[15] and conductimetry tests,[16,17] showing a two step ionization process, according to following scheme:

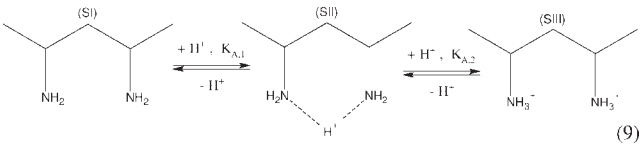

(9)

It is probable that the PVAm polymer evaluated in the present work does not show the two typical inflection points, which correspond to neutralization of two protonated species (SII and SIII in eq. (9), because it is a semi hydrolyzed polymer instead of a full hydrolyzed one as the polymer reported by the previous authors.

Moreover, in the Figure 3(a), the quantity of neutralized amine groups per polymer gram, which is determined on the inflection point (equivalence point), has a value equal to 7.3 ± 1 meq/g, this value is lower than value reported for PVAm obtained by full hydrolysis of poly(vinyl formamide) (23.20 meq/g,[5]). This result confirms the semi-

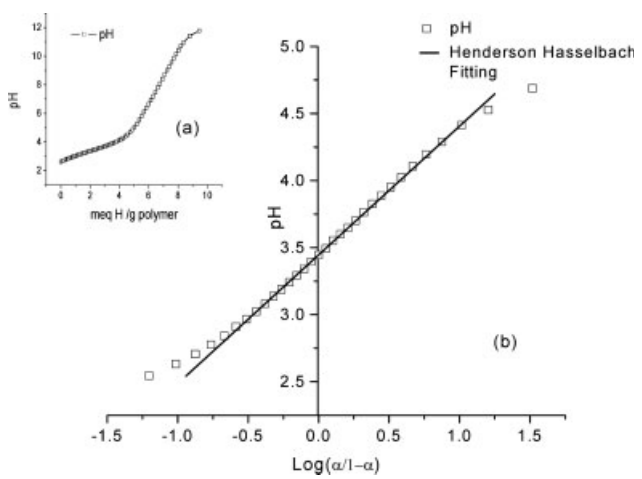

Figure 3 (a) Titration curve of the protonated poly(vinyl amine). (b) Henderson–Hasselbach plot for protonated PVAm titration curve.

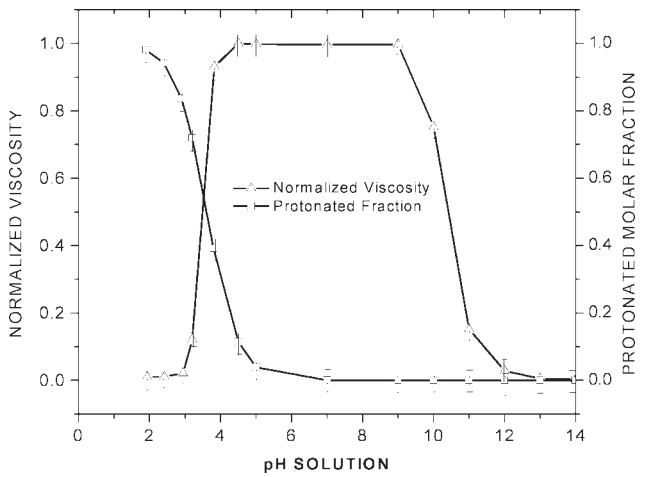

Figure 4 Protonated molar fraction of the amine groups and corresponding normalized viscosity.

hydrolyzed state of the PVAm employed. In this state there are nonhydrolyzed *N*-vinylformamide groups randomly distributed along the polymeric chain, which breaks the amine group continuity. Those groups represent a steric hindrance to Amine-Hydrogen complex generation (species SII), as a result only one step protonation process takes place (species SIII).

Figure 3(b) illustrates the titration curve analysis. Experimental data was fitting with the modified Henderson–Hasselbach model eq. (3), and an $m = 0.94$ value was determined. This value indicates that electrostatic interactions along the polymeric chain are not significant and confirms the steric hindrance of nonhydrolyzed *N*-vinylformamide groups that inhibits the formation of species SII. It is important to mention that in the previous works PVAm presented *m* values close to 5.34 with nonhydrolyzed *N*-vinylformamide groups content below to 1%.[16,17]

Besides, the pKa was determined as the origin ordinate of the straight line in Figure 3(b), which is valid for polyelectrolytes with low electrostatic interactions force ($m \approx 1$) between its polar functional groups and evaluated in a high ionic force solution (KCl 1M).[7,18] The value obtained is 3.46 ± 0.004, this value is lower than values reported in others works, pKa = 5.1.[15–17] This is also because of the semi-hydrolyzed state previously discussed, which produces a clear reduction on the electrostatic interactions along the polymeric chain.

With the pKa parameter and eq. (2), it is possible to predict the fraction of protonated and unprotonated amine groups. Figure 4 shows the evolution of the protonated and unprotonated fractions with the pH. Although all groups are protonated for pH < 2.2, their proportion decreases significantly at larger values of pH, until they almost disappear at pH > 6. It is important to note in Figure 4 that the increase of the normalized viscosity with the pH is correlated with the increase of the unprotonated amine fraction. Actually, the viscosity increases from a value of $1.3\ 10^{-3}$ Pa s at pH = 2, to a value of 1.5 Pa s at pH = 4. Once the viscosity attains a maximum at a pH of 4.5, it remains at a stable value until pH = 9, and then diminishes again down to the initial value. This behavior demonstrates that at a pH < 2.2: (i) the protonated amine groups do not react with the cupric sulfate, (ii) PVAm chains stay free and, (iii) the viscosity remains low. In contrast, when the amine groups become unprotonated by a pH increase, the copper salt reacts until exhaustion. For pH = 4.3 the viscosity stops increasing because all the cupric sulfate molecules have already reacted and no new links are created. Finally, for pH = 9 the concentration of OH^- ions is so large that the coordinate covalent bonds decompose into copper hydroxide and PVAm. Therefore, the viscosity diminishes to its original value. The corresponding reaction is given by eq. (10):

$$\mathrm{Cu[PVAm]_4} + \mathrm{OH^-} \longrightarrow \mathrm{Cu(OH)_2} + \mathrm{PVAm} \quad (10)$$

Moreover, Figure 5 illustrates the evolution of the color and homogeneity of the previous solution during the crosslinking reaction. Figure 5(a) shows the initial water solution of PVAm/HCl with a pH = 1, where the polymer is completely dissolved. A clear solution is formed without agglomerates, sediments, or foams. Figure 5(b) shows the same solution after the cupric sulfate is added, a green solution is formed; this color is characteristic of solutions with free copper ions. Figure 5(c–f) show the aspect and color of the solution when the pH is increased by adding NaOH. In Figure 5(c) the color changes from green to blue, and a slight volume contraction is noticed; both phenomena are because of the start of the crosslinking reaction. Finally, the blue color of the solutions obscures as the pH continues to increase. At a pH = 5 the color is almost black and the reaction is finished.

According to results reported by Liu et al.,[3] and Ludovic et al.,[19] the cross-linking reaction can be represented by eq. (11):

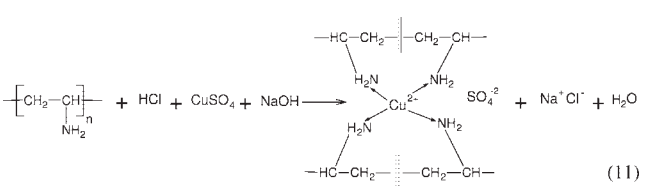

(11)

The crosslinking (chelating) reaction is produced by the sp^3 hybridization of the nitrogen atom of the amine groups. The electrons of the amine group are bonded to the "*d*" orbitals of the copper ion to form a complex. It is for this reason that this reaction

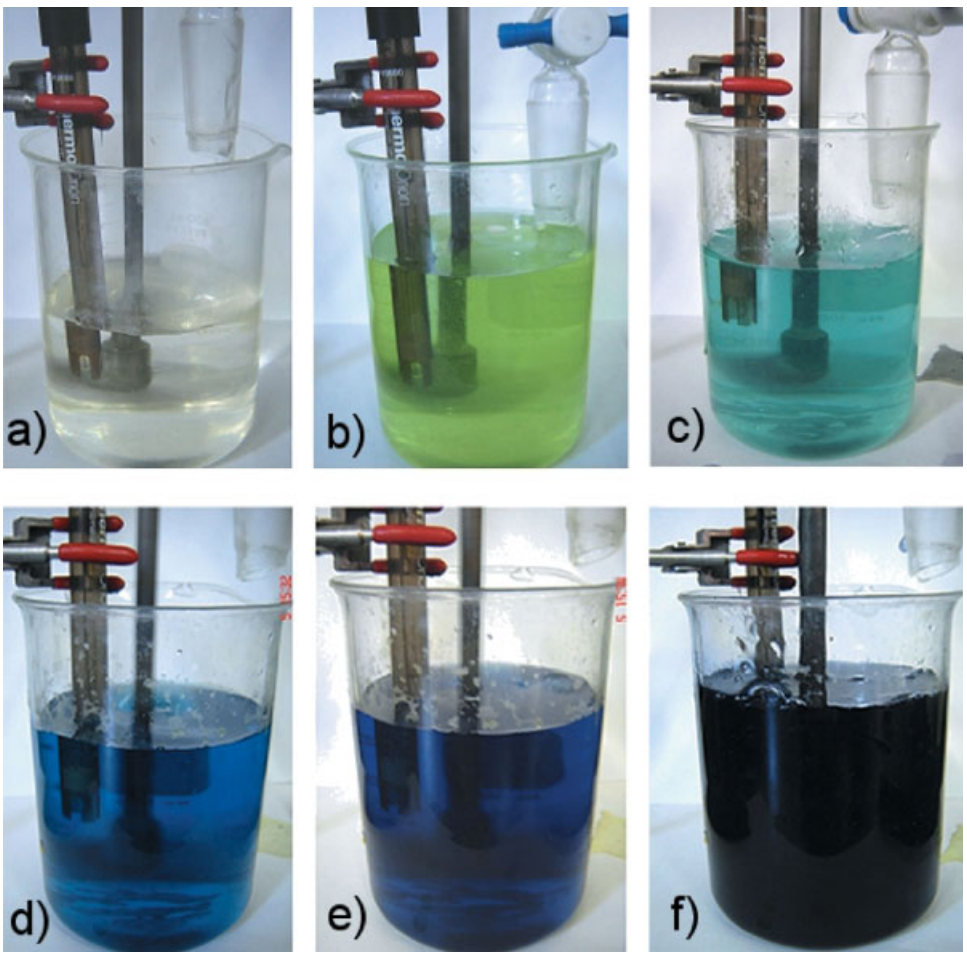

Figure 5 (a) Initial; PVAm/HCl solution with a pH = 1; Afterward PVAm/HCl solutions added with 1% of cupric sulfate and adjusted pH to: (b) 1.0; (c) 1.9; (d) 2.5; (e) 3.5 and (f) 5.0 by addition of sodium hydroxide solution. [Color figure can be viewed in the online issue, which is available at www.interscience.wiley.com.]

depends strongly on the acidity of the solution. At low pH values, the chelating reaction occurs with the hydrogen atoms in the solution preferentially, and therefore the crosslink reaction does not take place. At pH between 2.5 and 9, the molar concentration of deprotonated amine groups is increased and crosslinking reaction occurs, and an increase in the viscosity is shown because of the reticulation process. Similarly, at high pH levels, the concentration of OH^- is larger and copper ions start forming copper hydroxide instead of forming complex crosslinking bonds. Those phenomena permit controlling this fast reaction by manipulating the solution pH.

After drying the material obtained was extruded to fabricate the Type I and II samples described in the experimental section. It is important to note that common hydrogels, which are crosslinked by covalent bonds, are destroyed by temperature and shear stress during extrusion. Actually, those hydrogels cannot flow in an extruder without major degradation, because the crosslinking bonds between the polymer molecules are first order bonds, normally covalent, and they are not re-established after heating or flow. Therefore, the reticulated network is destroyed when it is heated and forced to flow. However, in the present case the bond produced by chelation is a second order bond, which may be re-established after thermal activated flow. Therefore, when the material is heated, the free volume between molecules increases and their interaction with the copper ions diminishes permitting their flow. But, when the material is cooled the free volume diminishes and the crosslinks strength is re-established reforming the reticulated network. To evaluate the veracity of the previous assumption, we have evaluated the gel fraction before and after the extrusion process at 140°C. The results are reported in Table II (in this Table the water uptake and crosslinking density of the formulations after processing are also reported.) It is important to observe that the gel fraction obtained is practically the same before and after extrusion. This fact shows that actually the chelating bonds are recovered after thermal activated flow in an extruder. This characteristic makes

TABLE II
Structural Parameters of the Formulations Studied

Formulation	Cupric sulfate crosslinking agent (wt %)	Gel fraction before processing	Gel fraction after processing	Water uptake, M_f/M_0	Polymer volume fraction in equilibrium in swollen network, ϕ	Crosslinked Density, ρ_c (10^{-2})
A	0.07	0.95 ± 0.005	0.94 ± 0.005	11.10 ± 0.05	0.0900	0.309 ± 0.004
B	0.25	0.96 ± 0.005	0.96 ± 0.005	9.900 ± 0.05	0.1010	0.334 ± 0.004
C	0.49	0.99 ± 0.005	0.98 ± 0.005	8.901 ± 0.05	0.1123	0.367 ± 0.04

this type of crosslinking ideal to produce hydrogels suitable to be processed by standard methods (extrusion, injection, etc.)

Figure 6 shows the kinetic of water absorption of each formulation. It is observed an almost linear behavior until 250 min have passed, after which an asymptotic evolution is followed. The water uptake is among 9 to 11 times greater than their original weight. Even though this water uptake is not impressive (there are hydrogels capable to absorbing water fifty or even more times their weight), it is enough for our purposes.

To describe the water diffusion mechanism inside our polymer, the following equation based on power law model is applied[20–22]:

$$F = \frac{M_t}{M_i} = Kt^n \tag{12}$$

Where M_t and M_i are the mass of water absorbed at time t and mass of water absorbed at equilibrium, respectively, K is a constant related to gel structure, n is the diffusion exponent and t is the time. Moreover, the diffusion coefficient is calculated by[23]:

$$D = \pi r^2 \left(\frac{K}{4}\right)^{\frac{1}{n}} \tag{13}$$

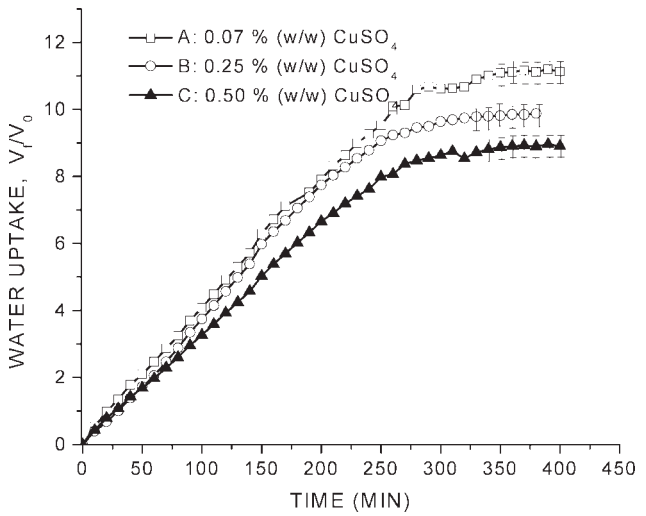

Figure 6 Water uptake of the three formulations studied.

Where r is the sample radius and D is the diffusion coefficient that is reported in Table III. According to the power law model, there are two water diffusion mechanisms: when $n = 0.5$ which corresponds to Case I or Fickian diffusion and $n = 1$ called Case II diffusion.[20] When $0.50 < n < 1$, the mechanism diffusion is called anomalous diffusion.[24] It is noted from the results reported in Table III, that the diffusion exponent is practically equal to 1.0, therefore the water diffusion in our polymer can be described as a Case II diffusion, with no dependence of the copper content.

The crosslinking density, ρ_c, was calculated using eq. (5). However, to perform this calculation is necessary to evaluate the interaction parameter χ_{12} for the system PVAm–water, because currently there is no data about its value in the literature. As previously mentioned this parameter may be evaluated by viscosimetry employing the Kramer and Huggins eqs. (6 and 7), at theta temperature. Figure 7 illustrates the Huggins and Kraemer graphs for PVAm–water system evaluated at 25°C. A resume of the respective parameters of this model measured at different temperatures is presented in the Table IV. As previously mentioned, the theta temperature is assessed at the point where the slope of the straight line described by the Kramer equation is close to zero; or, in other words, where the absolute value of the parameter $K_k[\eta]^2$ of this equation is minimum. Figure 8 shows the behavior of this last parameter when solution temperature changes. It is noticed that the theta temperature for the system PVAm - water is practically equal to 25°C.

The average value of interaction parameter computed at 20, 30, and 35° C, using the data of Table III and eq. (8), is $\chi_{12} = 0.445 \pm 0.005$. This parameter indicates the affinity among solvent and polymer;

TABLE III
Values of n y K for the Studied Formulations Obtained by Swelling Tests

Formulation	K (min^{-1})	n	D·10^{-4} (cm^2/s)
A	0.0048 ± 0.00030	0.943 ± 0.0122	3.19 ± 0.0122
B	0.0028 ± 0.00018	1.065 ± 0.0122	6.05 ± 0.0131
C	0.0038 ± 0.00018	0.993 ± 0.0122	4.21 ± 0.0093

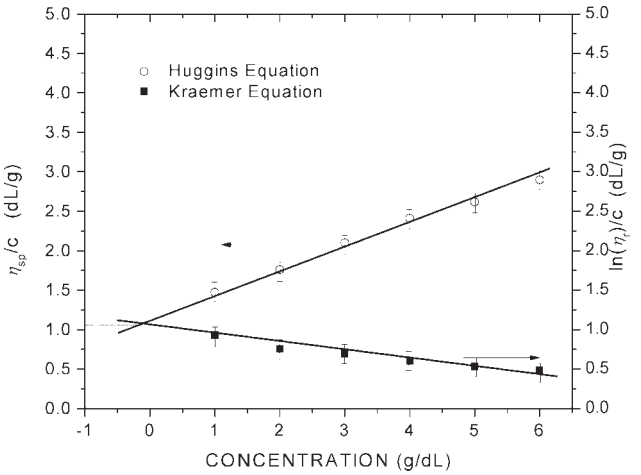

Figure 7 Determination of intrinsic viscosity at the point of common intercept between straight lines of Kraemer (5) and Huggins (6) plots.

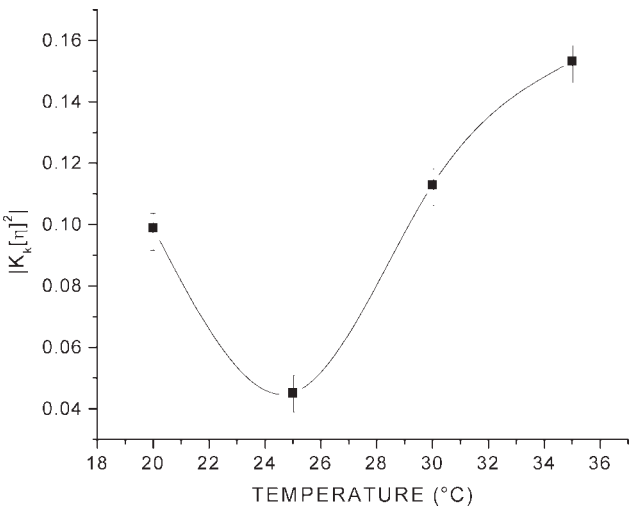

Figure 8 Evolution of the straight line slope, $K_k[\eta]^2$, described by the Kramer eq. (5).

values among 0 to 0.50 establish high compatibility between solvent and polymer.[13] For the present case, hydrophilic interactions like hydrogen bonds exist because of the presence of amine groups, which promotes the water absorption observed.

Employing the data reported in Table II, the Flory–Huggins interaction parameter χ_{12} and eq. (5); the crosslinking densities were assessed. The densities obtained were: $0.309 \pm 0.05 \times 10^{-3}$, $0.334 \pm 0.05 \times 10^{-3}$, and $0.367 \pm 0.05 \times 10^{-3}$, for the three formulations studied; A, B, and C, respectively. All the structural parameters calculated are summarized in the same Table II.

Figure 9 shows the FTIR absorbance spectra of the previous formulations. We are interested in two peaks; the first one upon 1590 cm^{-1}, which corresponds to vibrations of the type "scissoring" of the group —NH_2, and a second peak upon 1350 cm^{-1}, which is because of the vibrations of the type "stretch" of the link C—N. It is observed that while the peak at 1590 cm^{-1} remains unchanged, a notable depression and shift of the peak at 1350 cm^{-1} are observed. This depression and shift, is apparently produced by the presence of covalent coordinated links from the chelating reaction, which restrains the movement of the groups amino and therefore, the capacity of vibration of them reducing the quantity of energy that the substance is capable of absorbing at the corresponding frequency. Finally, the collapse of the peak at 1350 cm^{-1}, when just a content of 0.07 wt % of cupric sulfate is integrated, is an interesting phenomenon that unfortunately is unclear for us at the present time.

Moreover, TGA tests were performed to evaluate the polymer thermal stability. Figure 10 illustrates those tests. A first zone is observed from 25°C to almost 180°C, corresponding to loss of the chemiabsorbed water. After this point the PVAm/Cu(II) formulations start to decompose, being the formulation C the more stable. At about 180°C the neat PVAm decomposes until a temperature between 420 and 560°C where the polymer is practically calcinated. It is observed that the thermal effect of this type of crosslinking increases significantly the thermal stability of this polymer, permitting to extrudate it without degradation at a processing temperature of 140°C.

To evaluate the processability of the crosslinked formulations, their viscosity has been measured at 140°C. The results are reported in Figure 11. A pseudo plastic power law behavior is observed in the range of shear rates tested. The formulation C is evidently the more viscous because it is the most crosslinked. It is important to note that at a shear rate of 1 s^{-1} the viscosities of the crosslinked formulations are in the range between 105 KPa s and 115 KPa s; with such viscosities, we can extrudate those formulations in an optimum way. However,

TABLE IV
Experimental Parameters of the Kramer and Huggins Equations

Temperature (°C)	[η] (dL/g)	K_k	K_H	$-K_k[\eta]^2$
20	1.27 ± 0.005	0.061 ± 0.0005	0.219 ± 0.0005	0.099 ± 0.0005
25	1.13 ± 0.005	0.066 ± 0.005	0.274 ± 0.0005	0.0452 ± 0.0005
30	1.47 ± 0.005	0.052 ± 0.005	0.177 ± 0.0005	0.113 ± 0.0005
35	1.72 ± 0.005	0.0521 ± 0.005	0.154 ± 0.0005	0.153 ± 0.0005

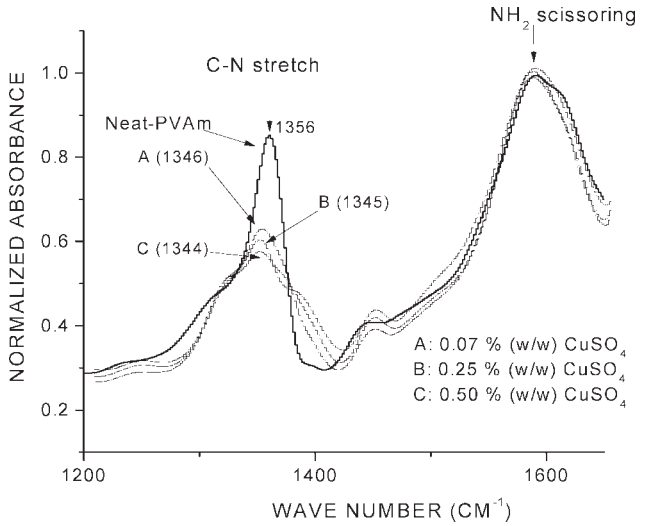

Figure 9 FTIR absorption spectra of the three formulations studied and neat PVAm.

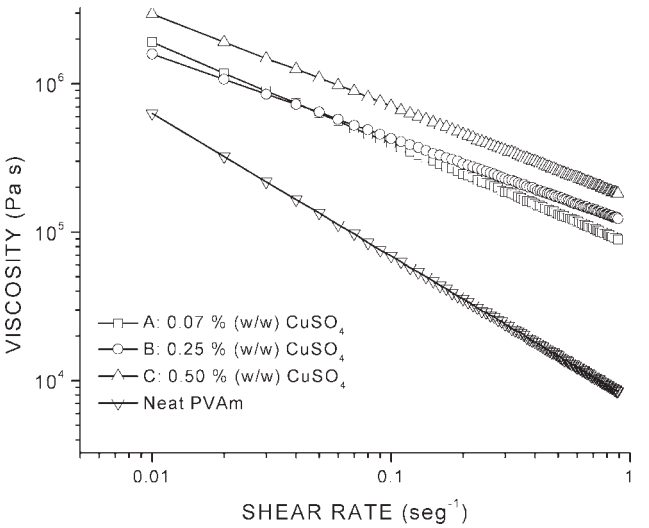

Figure 11 Viscosity vs. shear rate for the three formulations studied and neat PVAm.

we chose to add about 5 wt % of 1, 2, 3 propanetriol (TPG for short) to each formulation as a plasticizer to facilitate the extrusion process.[25]

Concerning the electrical behavior of different formulations, the results of both types of tests (I and II) are reported in Figures 12 and 13. In those Figures the changes of their normalized apparent resistivity, ρ_r/ρ_{ro}, when samples are dipped in water, is shown. (All the samples were submerged in water at t = 5 s, during 25 s). In a initial interval of 5 s, the system steady state is indicated on those figures (this interval is drawn just as a reference, because the actual transient period of the circuit-sample system can take some minutes). After exactly 5 s, samples were dipped in water. First of all it is important to observe that the rate at which formulations A and B switch from their high original resistivities ($\sim$ 200 KΩ cm) to lower ones ($\sim$ 10 KΩ cm), takes less than 1 s, which make them suitable materials to design ultrafast water sensors. Also, it is important to note that no differences are observed between the behavior of samples Type I and II. On the other hand, formulation C is significantly slower; this is evidently due to a slower diffusion of water into a material with a larger crosslinking density, also, an erratic behavior of their samples is noted with Type I geometry (Fig. 14) because of inhomogeneous water diffusion and electrical connection instabilities produced by swelling.

Figure 14 shows SEM micrographs for three different formulations where micromorphology of extruded material is analyzed. Samples from formulations A and B have a notable porosity, whereas formulation C presents a slightly less porosity. This last analysis permits to explain the fast electrical switch observed in the first two formulations, which can be mainly due to water penetration into material

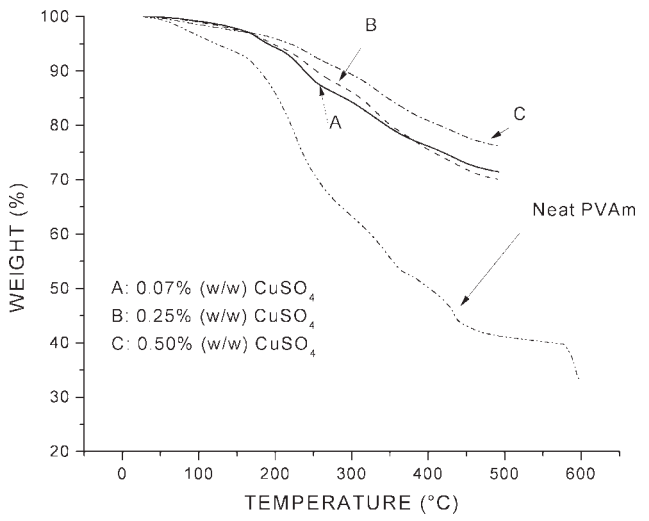

Figure 10 TGA results of the three formulations studied and neat PVAm.

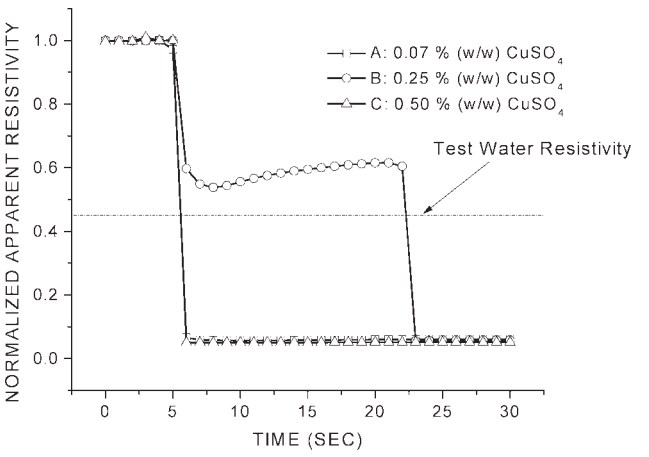

Figure 12 Normalized resistivity vs. immersion time for the three formulations studied, employing samples Type I.

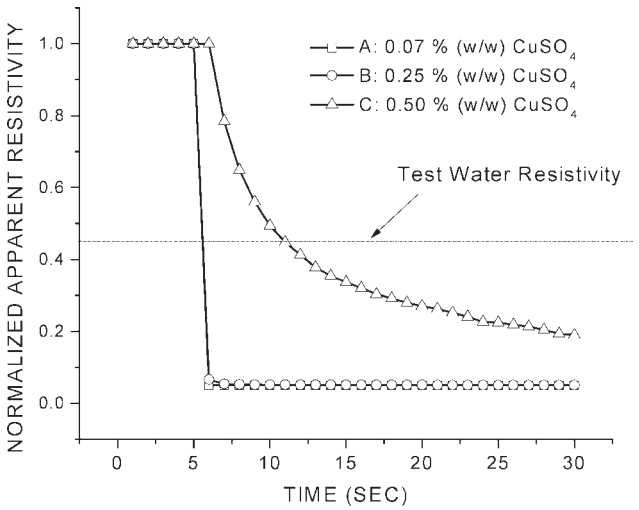

Figure 13 Normalized resistivity vs. immersion time for the three formulations studied, employing samples Type II.

by capillary transportation, rather than by diffusion and swelling,[26–28] interconnecting electrically conductive pathways and reducing almost instantaneously the apparent polymer resistivity. Therefore electrical switch rate may be more associated to capillary transportation phenomena (apparent diffusion coefficients close to 106 cm2/s[24,27,28]) than to simple diffusion (diffusion coefficient close to 10^{-4} cm^2/s, see Table III.) Also, it is for this reason that we have plotted in the abscise of graphs of Figures 12 and 13 an apparent resistivity, because it is not the actual resistivity of the material, but this macroscopically obtained as a result of the previous transport mechanisms.

Also, it is interesting to observe that the final resistivity of all samples is lower that the resistivity of potable water employed in those tests ($\sim$ 90 KΩ cm). Therefore, a notable evidence of ionic conductivity is manifest. This extra conductivity is attributed to disperse NaCl salt into polymer matrix, and to hydrogen ions transportation by means of amine groups which can accept or donate protons through polymer matrix because of their acid-base behavior.[29,30]

Figure 15 shows the electrical response of the Type II test samples, made with formulation A, when they were subjected to swelling and deswelling tests with water. In a first cycle, when the sensor is exposed to water, an extreme fall in its apparent resistivity is registered, in contrast, the deswelling (drying) is slow taking close to 120 min (deswelling was realized in a humidity and temperature controlled chamber at 30% RH and 25°C). Nevertheless, in a second cycle, the deswelling rate is five times faster than at the first cycle, during 20 min in same conditions of humidity and temperature, and in a third cycle, deswelling is practically the same.

This behavior is attributed to an increase in the number and size of pores during swelling–

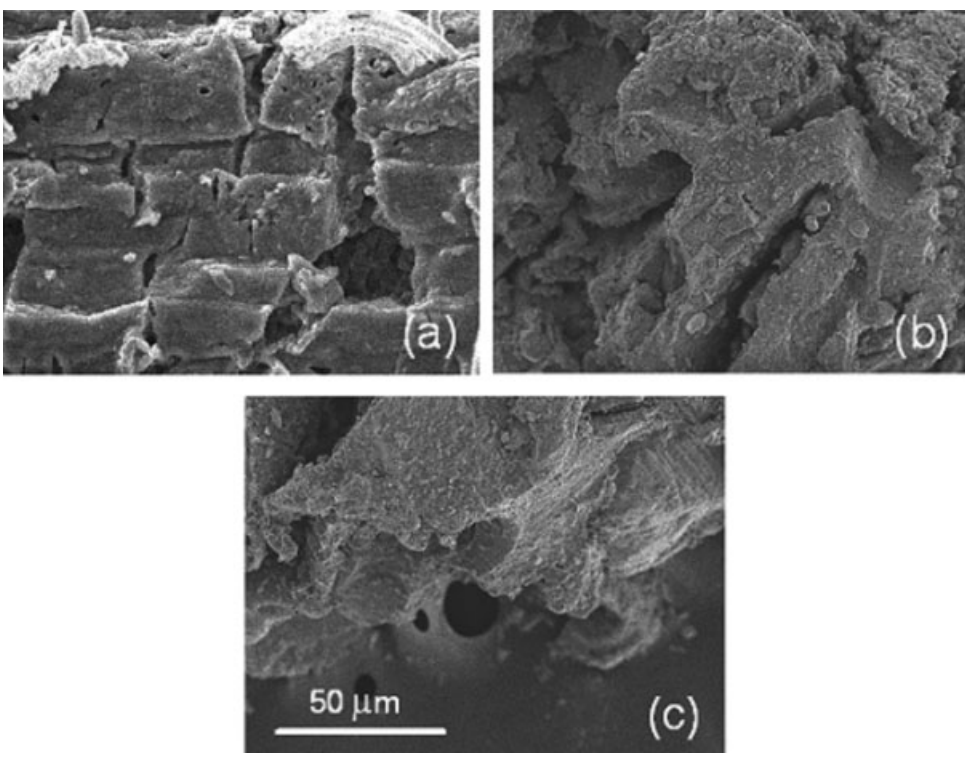

Figure 14 SEM characterization samples surfaces. (a) Formulation A: 0.07% (w/w) $CuSO_4$, (b) Formulation B: 0.25% (w/w) $CuSO_4$ and, (c) formulation C: 0.50% (w/w) $CuSO_4$.

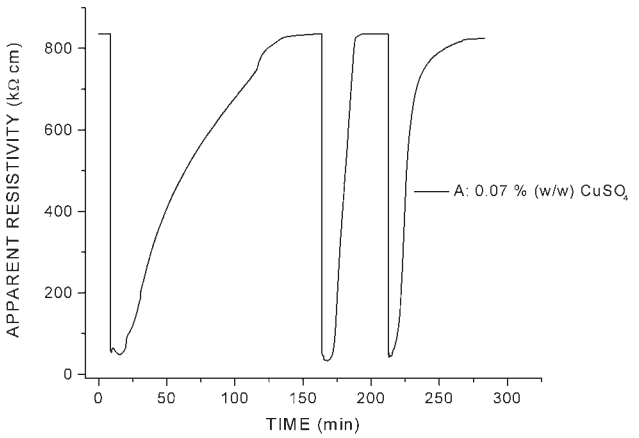

Figure 15 Electrical response of a sample prepared with formulation A: 0.07% (w/w) $CuSO_4$, when it was subjected to swelling and deswelling test. The exposition time was 5 min and deswelling event was realized at 30% HR and 25°C.

deswelling tests. In the swelling step the water expands the polymer matrix increasing the number of diffusive pathways. Afterward, in the deswelling step, water diffuse out of polymeric matrix leaving porosities that allow water to rapidly diffuse out of the polymeric matrix in posterior cycles. To elucidate this hypothesis, Figure 16 shows the SEM micrographs of a cable sensor made with formulation A before and after swelling–deswelling tests where an apparent increasing of porosity is exposed. This observation confirms our previous assumptions.

Finally, it must be stressed out that the PVAm–Cu composites show repeatability on their electrical behavior with an electrical response that changes close to three magnitude orders between dry and wetted states, which is easy to detect with common measuring equipment. Therefore, this material is an excellent candidate for its application in distributed water sensors.

CONCLUSIONS

We have developed a methodology to reticulate PVAm employing a copper salt. This methodology provides a material that has a crosslinking degree large enough to be employed in water sensors, but not strong enough to make it impossible to be extruded. The hydrogels developed have an ideal micromorphology and structure which switch very

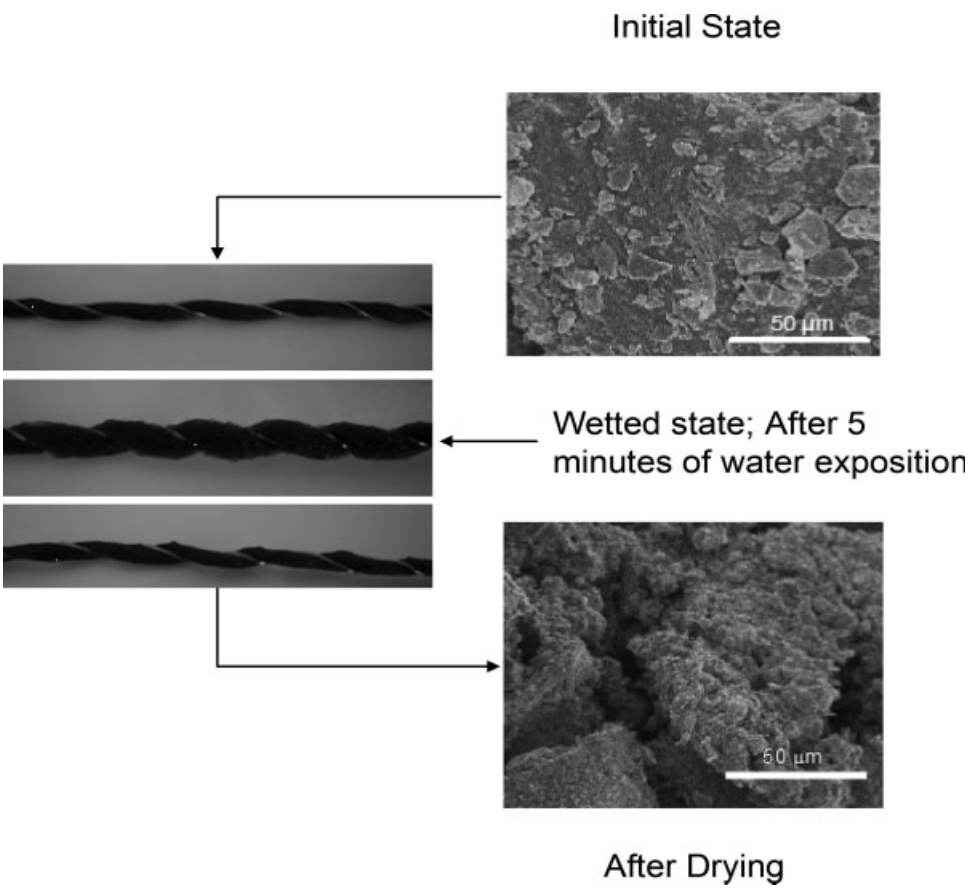

Figure 16 SEM micrographs of a sample prepared with formulation A: 0.07% (w/w) $CuSO_4$, when it was subjected to swelling and deswelling (drying) test.

fast from an isolate material to a conductive one when they enter in contact with water. The hydrogel prepared has a response time close to 5 s, which is shorter than typical sensors, which have a response time among 1 and 5 min, this characteristic is important to design water sensors for any special applications. The complex bonds formed between the Cu(II) ions and the amine groups of PVAm produce an interesting network of crosslinked structures that generate a microporous morphology when the material is extruded. This characteristic and the fact that this material swells notably by absorbing water are responsible for its fast electrical switch in the presence of humidity. Consequently, this material is an excellent candidate to produce ultrafast water sensors.

The authors thank Miguel Orozco and Claudia Hernandez for their technical support.

References

1. Mendoza-Payán, J. G.; Márquez-Lucero, A. IMPI, Mexico. Mexican Pat. 294,523, (2008).
2. Lu, J. L.; Zhang, Z. Q.; Xia, X. W.; Wang, L. H.; Zhu, X. L. J Mol Catal A 2004, 207, 205.
3. Liu, M.; Yan, X.; Liu, H.; Yu, W. React Funct Polym 2000, 44, 55.
4. Martell, A. Coordination Chemistry, ACS Monograph 174; American chemical society: Washington D.C., 1978; pp 159–165.
5. BASF Corporation, Lupamin® 9095 High Molecular Weight Linear Poly(vinyl amine) 2002, Technical Bulletin, available at: http://www.basf.com/performancechemical/pdfs/Lupamin_9095.pdf#search=%22lupamin%209095%22. Accessed on 7th September 2006.
6. Day, R.; Underwood, A. Quantitative Analysis, 5th ed.; Prentice Hall: New York, 1989; pp 225–258.
7. Laguecir, A.; Ulrich, S.; Labille, J.; Fatin, N.; Stoll, S.; Buffle, J. Eur Polym J 2006, 44, 1135.
8. Mitsukami, Y.; Hashidzume, A.; Yusa, S.; Morishima, Y.; Lowe, A.; Mccormick, C. Polymer 2006, 47, 4333.
9. Jeffery, G.; Basset, J.; Mendham, J.; Denney, R. C. Vogel's Textbook of Quantitative Chemical Analysis, 5th ed.; Longman, Scientific and Technical, Wiley: New York, 1989; pp 35–42.
10. Flory, P. J. Principles of Polymer Chemistry; Cornell University: Ithaca and London, 1953; p 357.
11. Yamakawa, H. Modern theory of Polymer Solutions; Harper and Row: New York, 1971; pp 124–135.
12. Ovejero, G.; Perez, P.; Romero, M. D.; Guzman, I.; Diez, E. Eur Polym 2007, 43, 1444.
13. Yilmaz, F.; Cankurtaran, Ö. Polymer 1997, 38, 3539.
14. Brown, R. Handbook of Polymer Testing, Physical Methods; Marcel Dekker: New York, 1999; pp 617–647.
15. Chang, C.; Fish, F.; Muccio, D.; Pierre, T. Macromolecules 1987, 20, 621.
16. Kobayashi, S.; Do Suh, K.; Shirokura, Y. Macromolecules 1989, 22, 2363.
17. Sumaru, K.; Matsuoka, H.; Yamaoka, H. Macromolecules 1996, 100, 9000.
18. Koetz, J.; Kosmella, S. Polyelectrolytes y Nanoparticules; Springer: Berlin, Heidelberg, New York, 2007; pp 15–16.
19. Ludovic, J.; Morcellet, J.; Delporte, M.; Morcellet, M. Polym J 1992, 28, 1185.
20. Wu, S.; Li, H.; Chen, P. J Macromol Sci Polym Rev 2004, 44, 113.
21. Schott, H. J Macromol Sci Phys 1992, 31, 1.
22. Astarita, G. In Transport Phenomena in Polymer Systems, Mashelkar, R. A., Kamal, R., Eds.; Wiley: New York, 1989; pp 339–351.
23. Tuncer, K.; Likay, A. Eur Polym J 2006, 42, 1437.
24. El-Hamshary, H. Eur Polym J 2007, 43, 4830.
25. Vanin, F. M.; Sobral, P. J. A.; Menegalli, F. C.; Carvalho, R. A.; Habitante, A. M. Food Hydrocolloids 2005, 19, 899.
26. Mersano, E.; Bianchi, E.; Sciuto, L. Polym J 2003, 44, 6835.
27. Lévesque, S.; Lim, R. M.; Shoichet, M. S. Biomaterials 2005, 26, 7436.
28. Shiaw-Guang, H. D.; Jiunn-Nan Chou, K. Polym J 1996, 37, 1019.
29. Casalbore-Miceli, G.; Camaioni, N.; Li, Y.; Martelli, A.; Zanelli, A. Sens Actuators B 2005, 105, 351.
30. Casalbore-Miceli, G.; Yang, M. J.; Camaioni, N.; Maric, C.; Li, Y.; Sun, H.; Ling, M. Solid State Ionics 2000, 131, 311.